Expanded View Figures

Figure EV1. hTrmt13 is a human tRNA 2'-*O*-methyltransferase at position 4.

A Verification of the customized anti-hTrmt13. The ability of anti-hTrmt13 for immunoprecipitation in MDA-MB-231 cells assayed by Western blot (left). The protein level of hTrmt13 in WT and KO MDA-MB-231 cells assayed by Western blot using customized antibody of hTrmt13, GAPDH was used as control. A total 20 μg proteins of cell lysates were loaded.

B SDS–PAGE analysis of the purified hTrmt13. Standard molecular weights are shown on the left.

C The binding affinities of hTrmt13 for HctRNA^{Lys}(UUU), HctRNA^{Arg}(ACG), and HctRNA^{Phe}(GAA) analyzed by EMSA. The concentration of tRNAs is 0.15 μM.

D The capacity of HctRNA^{Gly}(GCC), HctRNA^{Lys}(UUU), HctRNA^{Arg}(ACG), and HctRNA^{Phe}(GAA) to be methylated by hTrmt13. Error bars represent mean ± SD for at least three independent experiments.

E The secondary structure of HctRNA^{Gly}(GCC) summarizing the mutations in A: U (U4A), C: G (U4C), and G:C (U4G) base pairs.

F The Um, Am, Cm, and Gm modification of HctRNA^{Gly}(GCC), U4A, and U4C and U4G mutants was detected by mass spectrometry after hTrmt13 incubation.

G Detection of Um4 in endogenous tRNA^{Gly}(GCC) or Cm4 in tRNA^{Gly}(CCC) using primer-extension assays. 40 μM or 0.5 μM dNTPs were used in the high or low dNTPs groups. The Nm modifications caused RT stop in low dNTPs groups, and the products (labeled by a star) are shorter than the RT read through products.

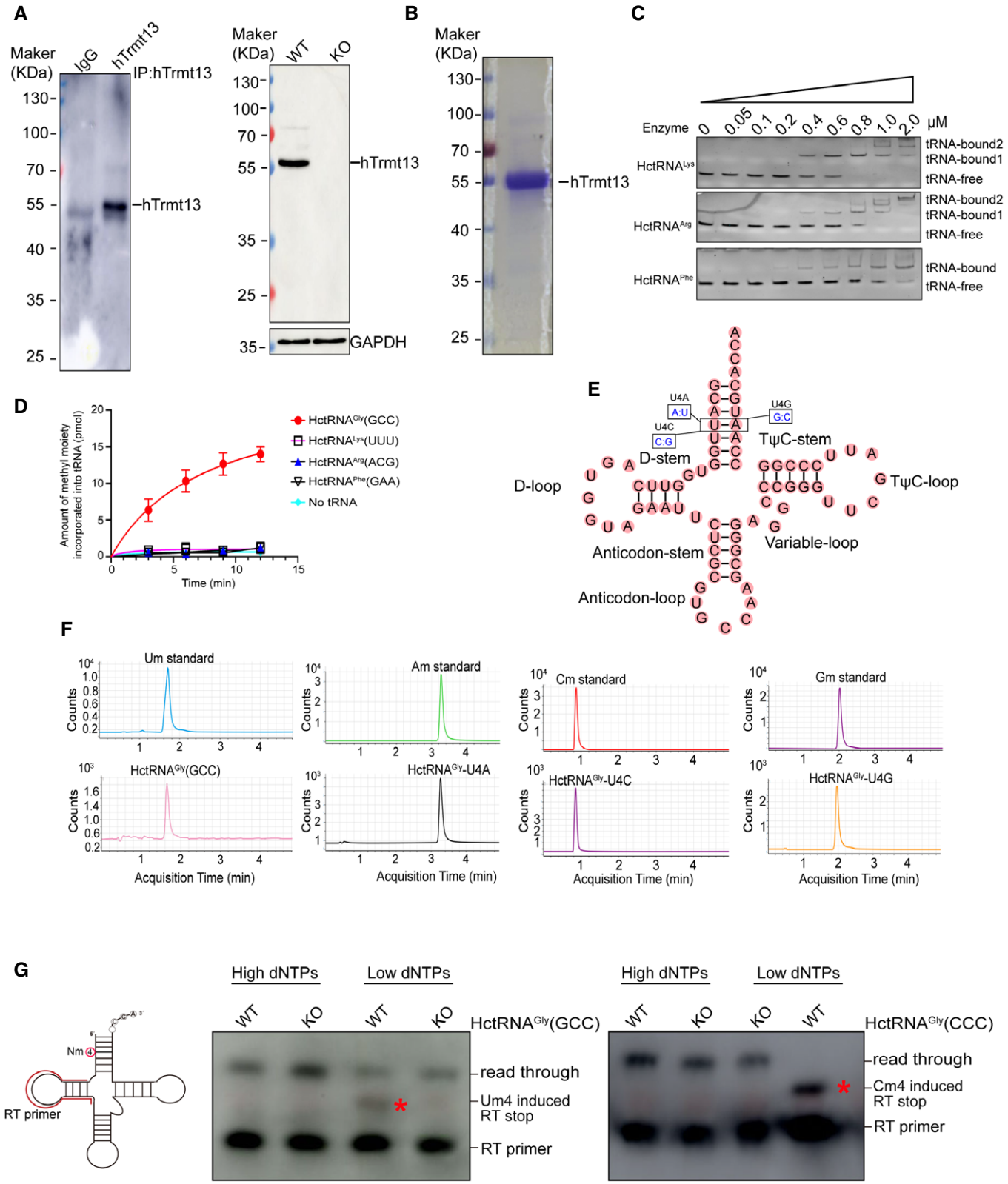
A
Maker (KDa)
IgG
hTrmt13
IP:hTrmt13
130
100
70
55
40
35
25
hTrmt13
Maker (KDa)
WT
KO
130
100
70
55
35
25
hTrmt13
35
GAPDH
B
Maker (KDa)
130
100
70
55
40
35
25
hTrmt13
C
Enzyme
0
0.05
0.1
0.2
0.4
0.6
0.8
1.0
2.0
μM
HctRNALys
tRNA-bound2
tRNA-bound1
tRNA-free
HctRNAArg
tRNA-bound2
tRNA-bound1
tRNA-free
HctRNAPhe
tRNA-bound
tRNA-free
D
Amount of methyl moiety incorporated into tRNA (pmol)
Time (min)
HctRNAGly(GCC)
HctRNALys(UUU)
HctRNAArg(ACG)
HctRNAPhe(GAA)
No tRNA
E
U4A
A:U
U4G
G:C
U4C
C:G
D-stem
TψC-stem
D-loop
TψC-loop
Anticodon-stem
Variable-loop
Anticodon-loop
F
Um standard
Am standard
Cm standard
Gm standard
HctRNAGly(GCC)
HctRNAGly-U4A
HctRNAGly-U4C
HctRNAGly-U4G
Counts
Acquisition Time (min)
G
Nm④
RT primer
High dNTPs
Low dNTPs
WT
KO
HctRNAGly(GCC)
HctRNAGly(CCC)
read through
Um4 induced RT stop
Cm4 induced RT stop
RT primer

Figure EV1.

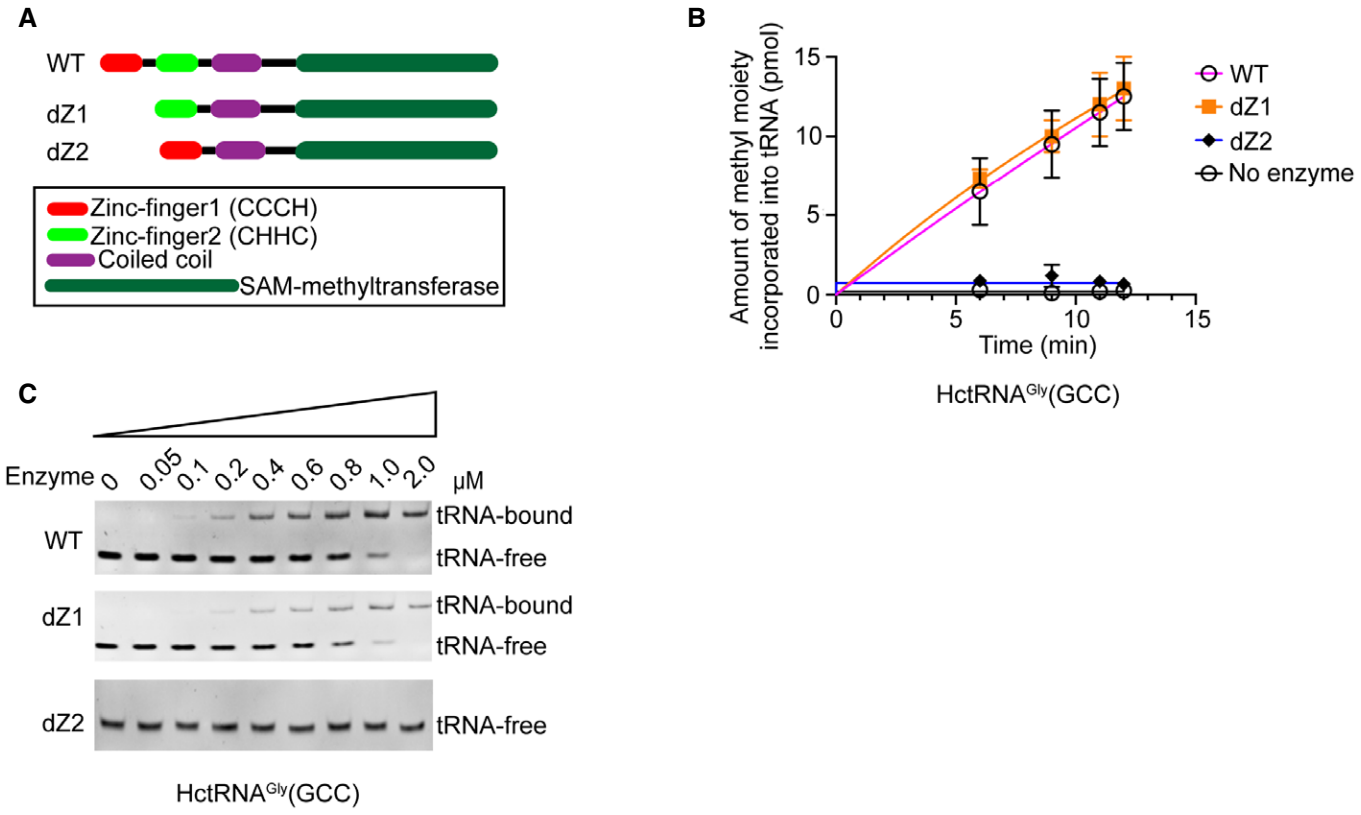

Figure EV2. The CHHC Zn-2 domain is crucial for hTrmt13 binding to tRNA.

A Schematic diagram of the primary structure of hTrmt13 summarizing the mutations. dZ1 indicates deletion of the CCCH Zn-1 domain, and dZ2 indicates deletion of the CHHC Zn-2 domain.

B The methyltransferase activities of hTrmt13 (WT) and its mutants (dZ1 and dZ2). For all experiments, three independent experiments were performed. Error bars represent mean ± SD for three independent experiments.

C The binding affinities of hTrmt13 and its mutants for HctRNA^{Gly}(GCC) (0.15 μM) analyzed by EMSA.

Figure EV3. Identification of catalytic inactive mutation of hTrmt13 and analyses of tRFs.

A Analysis of the TCGA dataset for the mRNA expression of hTrmt13 and EIF4A2 in breast cancer patients. Spearman order correlation analysis was performed.

B Schematic diagram of the primary structure of inactive hTrmt13 (E463A).

C The methyltransferase activities of hTrmt13 and E463A mutant toward HctRNA^{Gly}(GCC).

D The mRNA level of hTrmt13 in shSCR, sh-1, sh-2, sh+WT, and sh+E463A were detected by RT–qPCR.

E The polysome profiling of control (shSCR), hTrmt13 knockdown MDA-MB-231 cells (sh-1), and sh-1 with stable expression of hTrmt13 (sh-1+hTrmt13).

F Statistical analysis of the tRNA steady state levels assayed by northern blot.

G Statistical analysis of the *in vivo* aminoacylation level of hTrmt13 substrate tRNAs.

H Workflow of obtaining cDNA from tRFs by two methods (stem-loop method and Poly-A tail method). Small RNAs were enriched by mirVana™ miRNA Isolation Kit (Thermo Scientific). The reverse transcription primer of the stem-loop method consists of two parts: (1) universal stem ring structure and (2) reverse complementary bases with the target tRF. For the Poly-A method, Oligo Dt was used as the reverse transcription primer for Poly-A tail, which was tagged to small RNAs using QuantiMir™ Kit (SBI).

I RT–qPCR using a stem-loop primer to quantify the tRFs levels in shSCR, sh-1, and sh-2.

J Poly-A-based RT–qPCR to quantify the level of 5′-Gly-CCC in shSCR and sh-1.

K *De novo* protein synthesis in MDA-MB-231 cells transfected with different concentrations of 5′-Gly-CCC oligos.

L *De novo* protein synthesis in MDA-MB-231 cells transfected with different concentrations of HctRNA^{Gly}(CCC).

Data information: In C, D, F, G, I, J, statistical analysis was performed using *t*-tests. Error bars indicate mean ± SD for three independent experiments.

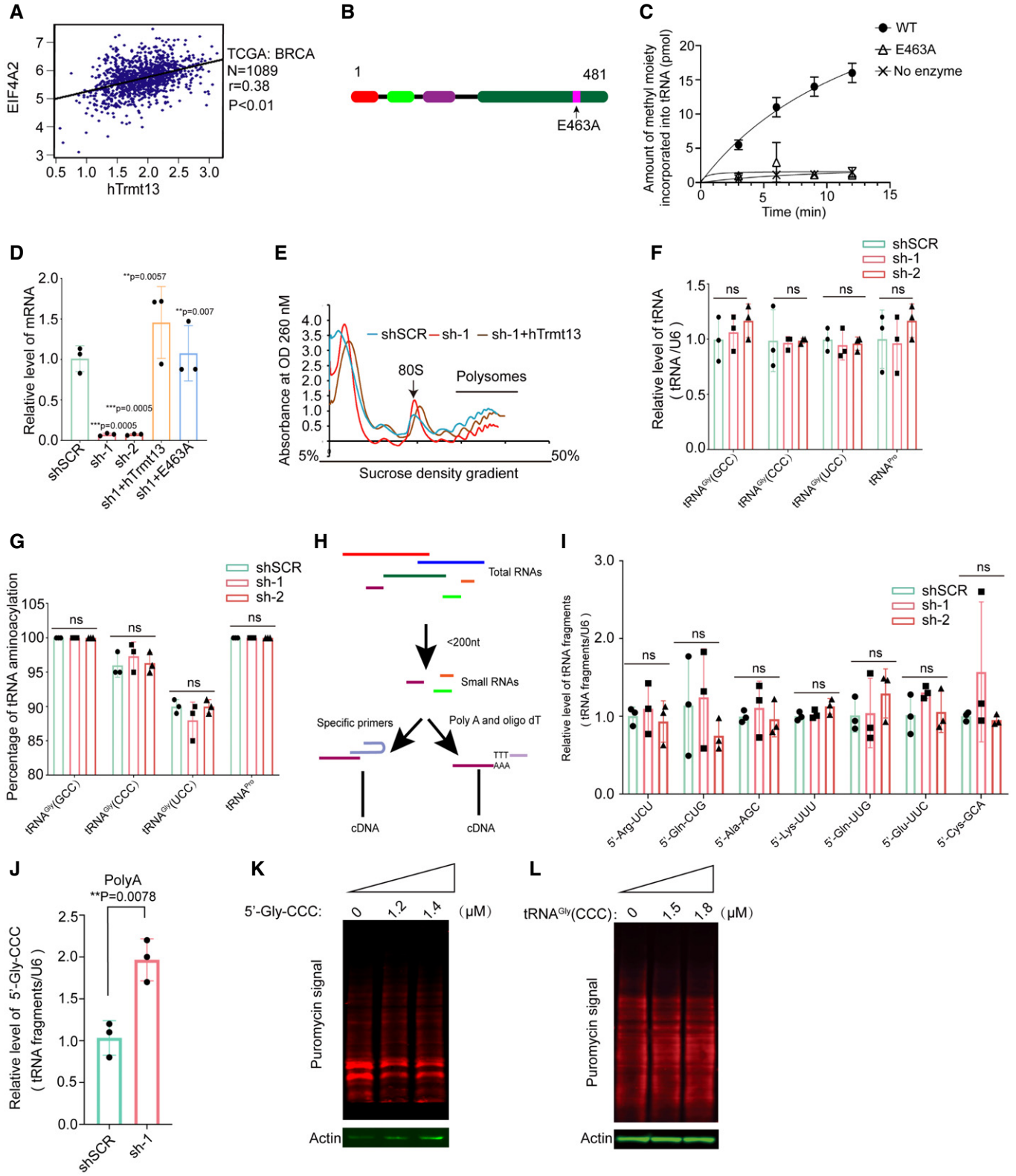
A
EIF4A2
hTrmt13
TCGA: BRCA
N=1089
r=0.38
P<0.01
B
1
481
E463A
C
WT
E463A
No enzyme
Amount of methyl moiety incorporated into tRNA (pmol)
Time (min)
D
Relative level of mRNA
**p=0.0057
**p=0.007
***p=0.0005
***p=0.0005
shSCR
sh-1
sh-2
sh1+hTrmt13
sh1+E463A
E
Absorbance at OD 260 nM
shSCR
sh-1
sh-1+hTrmt13
80S
Polysomes
5%
50%
Sucrose density gradient
F
shSCR
sh-1
sh-2
Relative level of tRNA (tRNA /U6)
ns
tRNAGly(GCC)
tRNAGly(CCC)
tRNAGly(UCC)
tRNAPro
G
shSCR
sh-1
sh-2
Percentage of tRNA aminoacylation
ns
tRNAGly(GCC)
tRNAGly(CCC)
tRNAGly(UCC)
tRNAPro
H
Total RNAs
<200nt
Small RNAs
Specific primers
Poly A and oligo dT
TTT
AAA
cDNA
cDNA
I
shSCR
sh-1
sh-2
Relative level of tRNA fragments (tRNA fragments/U6)
ns
5'-Arg-UCU
5'-Gln-CUG
5'-Ala-AGC
5'-Lys-UUU
5'-Gln-UUG
5'-Glu-UUC
5'-Cys-GCA
J
PolyA
**P=0.0078
Relative level of 5'-Gly-CCC (tRNA fragments/U6)
shSCR
sh-1
K
5'-Gly-CCC:
0
1.2
1.4
(μM)
Puromycin signal
Actin
L
tRNAGly(CCC):
0
1.5
1.8
(μM)
Puromycin signal
Actin

Figure EV3.

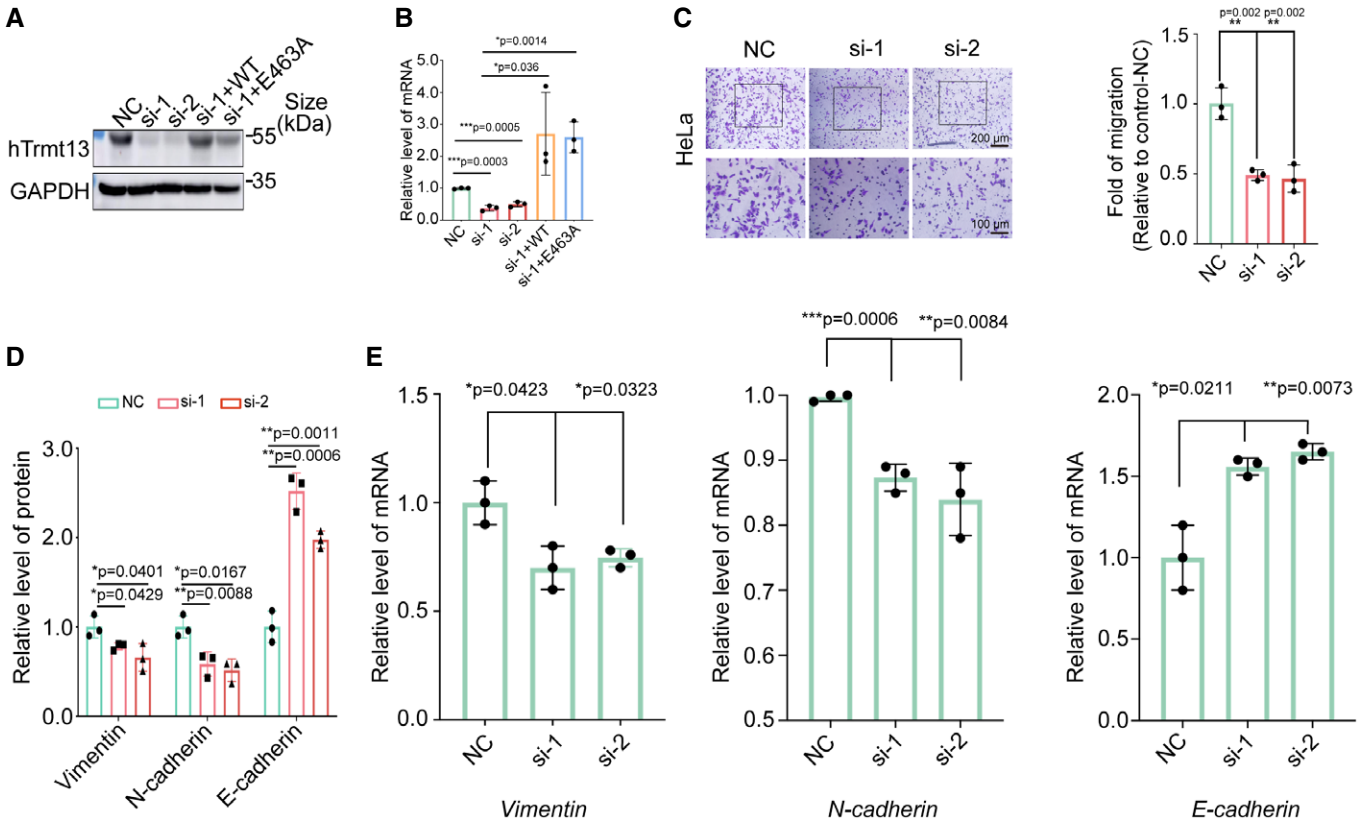

Figure EV4. hTrmt13 regulates cancer cell migration.

A, B Knockdown efficiency of hTrmt13 in MDA-MB-231 verified by Western blot (A) and by RT–qPCR (B).

C Transwell migration assays in HeLa cells infected with control siRNA (NC) or siRNA against hTrmt13 (si-1, si-2). Representative images (left) and statistical analysis (right) are shown. For each group, five different fields were chosen and counted using a microscope with 20-fold magnification.

D Statistical analysis of the expression of Vimentin, N-cadherin, and E-cadherin in control (NC) and hTrmt13 knockdown cells (si-1, si-2).

E RT–qPCR analysis of EMT-associated genes *Vimentin* (left), *N-cadherin* (middle), and *E-cadherin* (right) in hTrmt13 knockdown MDA-MB-231 cells compared to control.

Data information: In B–E, statistical analysis was performed using *t*-tests. Error bars represent mean ± SD for three independent experiments.

Figure EV5. hTrmt13 regulates *in vivo* cancer progression.

A, B GSEA plot showing interesting gene sets from MSigDB that were enriched for gene expressed higher in *hTrmt13* low group for SMID_BREAST_CANCER_HERBB2_UP (A) and enriched for gene expressed higher in *hTrmt13* high group for TURASHVILI_BREAST_DUCTAL_CARCINOMA_VS_DUCTAL_NORMAL_UP (B).

C Lung metastasis assay in mice model. MDA-MB-231-Luc-D3H2LN cells infected with lentivirus carrying control (shSCR) or shRNA against hTrmt13 (sh-2) were injected through the tail vein of 6-week-old female SCID mice (n = 4). Lung metastasis was monitored by bioluminescent imaging after three weeks of injection. Representative *in vivo* bioluminescent images are shown (left); bioluminescent quantitation of lung metastasis (right). Statistical analysis was performed using *t*-tests. Error bars represent mean ± SD from mice of shSCR or sh-2 groups.

D Immunohistochemical staining of 21 pancreatic carcinoma samples for hTrmt13 expression. Representative images are shown (left), and the mean staining intensity was analyzed by Image-Pro Plus software (right). Statistical analysis was performed using *t*-tests. Error bars represent mean ± SD from patient samples.

E TCGA analysis of the relationship between the overall survival time (OS) of liver cancer patients (LIHC, left, n = 277 (low)/88 (high), http://ualcan.path.uab.edu/analysis.html), patients with kidney renal clear cell carcinoma (KRIC, right, n = 260 (low)/259 (high), http://linkedomics.org/admin.php), and their expression of hTrmt13 using TCGA online analysis website.

F Kaplan–Meier survival analysis (http://kmplot.com/analysis/) of Kaplan–Meier plotter for the relationship between relapse free survival (RFS) of breast cancer patients and their expression of *TGFB1* (n = 2537 (low)/2392 (high)), *PKN2* (n = 3025 (low)/1904 (high)), or *MEF2A* (n = 1307 (low)/3622 (high)).

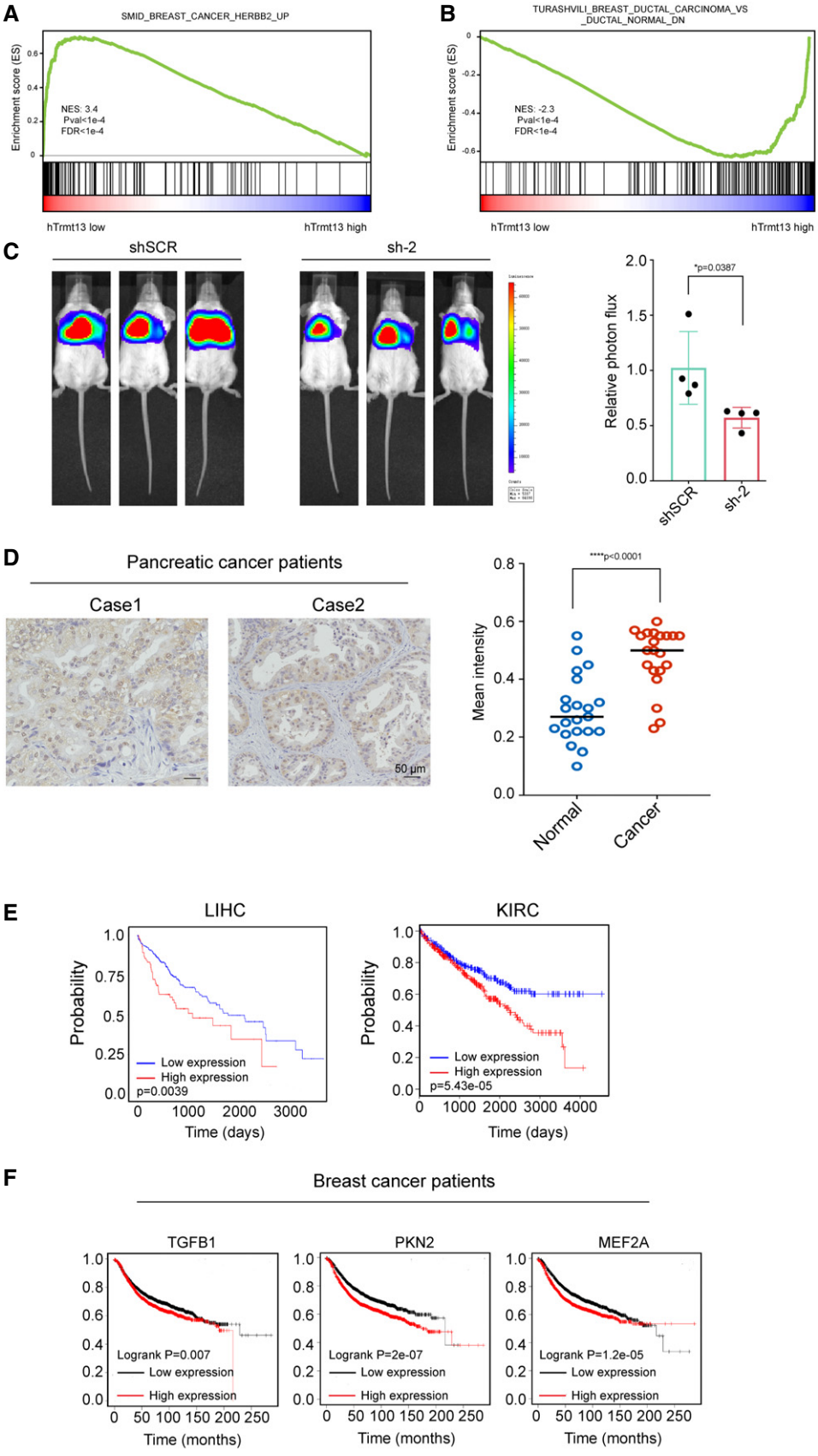

Figure EV5.